Monthly Notices of the ROYAL ASTRONOMICAL SOCIETY
MNRAS **488,** 910–917 (2019) doi:10.1093/mnras/stz1608

The cause of an extended recovery from an ICME-induced extreme geomagnetic storm: a case study

Anil N. Raghav,[1★] Komal Choraghe[1] and Zubair I. Shaikh [2★]
[1] *University Department of Physics, University of Mumbai, Vidyanagari, Santacruz (E), Mumbai-400098, India*
[2] *Indian Institute of Geomagnetism (IIG), New Panvel, Navi Mumbai-410218, India*

Accepted 2019 May 31. Received 2019 May 7; in original form 2019 February 8

ABSTRACT

Geomagnetic storms are crucial phenomena during severe space-weather conditions, which directly or indirectly affect communication, navigation, transportation, power grid and satellite electronic systems. They are usually caused by coronal mass ejections (CMEs) and/or corotating interaction regions (CIRs) of interplanetary space. The Earth's magnetic shield is weakened during a geomagnetic storm, which allows interplanetary plasma to penetrate inside the magnetosphere, further affecting the ionosphere as well as the upper atmosphere. Mostly, CMEs generating severe/extreme magnetic storms recover within one or two days. However, here, we demonstrate a case study of a particular extreme geomagnetic storm caused by a CME that exhibits a longer recovery phase than usual. The SYM-H index decreased to min ~-305 nT and recovered to ~-165 nT within $\sim$2.5 h. However, further recovery of the storm suddenly slowed down, i.e. $\sim$0.79 nT h^{-1}, and eventually took $\sim$4.5 d. This typical feature of recovery is not expected with CME-induced storms and further threatened us with various hazardous effects. The present study suggests that the possible causal agent for such extended recovery of the storm is the Alfvén wave. The study implies that Alfvén waves not only extend the recovery times of weak or moderate storms but also contribute to slowing down the recovery of severe/extreme storms.

Key words: coronal mass ejection (CME) – magnetohydrodynamics (MHD) – Alfvén wave – geomagnetic storm.

1 INTRODUCTION

Geomagnetic storms, which have paramount importance in space-weather studies, are extraordinary disturbances in the magnetosphere, usually defined as variations in the ground-based low-latitude geomagnetic horizontal field component (Chapman & Bartels 1940; Rostoker & Fälthammar 1967; Tsurutani & Gonzalez 1987; Gonzalez et al. 1994; Gonzalez, Tsurutani & De Gonzalez 1999; Echer & Gonzalez 2004; Echer et al. 2005a,b, 2008; Tsurutani et al. 2006a). During storms, energetic particles injected into magnetosphere from the solar wind have direct access to the Earth's ionosphere and upper atmosphere, which can disrupt the electronics of satellites (Shelley, Johnson & Sharp 1972; Laštovička 1996; Förster & Jakowski 2000), navigation and telecommunication systems, and high-potential power grids that can black out entire cities (Foster & Tetenbaum 1991; Thomson et al. 2005; Rao et al. 2009); in fact, their direct and indirect effects can engender a threat to the global economy (Oughton et al. 2017).

The southward interplanetary magnetic field (IMF) B_z component in the solar wind is the primary cause of geomagnetic storms (Rostoker & Fälthammar 1967; Gonzalez & Tsurutani 1987; Tsurutani et al. 1988; Gonzalez et al. 1994). The magnetic reconnection between the southward-directed IMF and Earth's northward-pointing magnetic field allows energy and plasma transfer between the solar wind and Earth's magnetosphere (Dungey 1961; Gonzalez & Mozer 1974; Akasofu 1981). In general, on the basis of the *Dst* and/or SYM-H index values, geomagnetic storms are divided into four different sets, i.e. weak (>-50 nT), moderate (-50 to -100 nT), strong/intense (-100 to -200 nT) and severe/extreme (<-200 nT) (Gonzalez & Tsurutani 1987; Gonzalez et al. 1994; Tsurutani et al. 1995a; Gonzalez et al. 1999; Zhang et al. 2007; Echer et al. 2008).

The study of the geomagnetic storm dependence on the solar cycle is used for clear and better understanding of various sources of geomagnetic storms. During the solar maximum phase, the Sun's activity is highly dominant by erupting coronal mass ejections (CMEs) (Gonzalez et al. 1999; Tsurutani et al. 2006a). Most of the intense and extreme/severe storms have been observed during a solar maximum phase, which are often associated with interplanetary CMEs (ICMEs) (Tsurutani et al. 1988, 1992; Gonzalez et al.

★ E-mail: raghavanil1984@gmail.com (ANR); zubairshaikh584@gmail.com (ZIS)

1999; Zhang et al. 2007; Echer et al. 2008). The ICMEs have two distinct substructures, i.e. magnetic clouds and sheath regions, which also modulate the cosmic ray intensity. (Gonzalez et al. 1999; Huttunen et al. 2006; Pulkkinen et al. 2007; Raghav et al. 2014, 2017; Shaikh, Raghav & Bhaskar 2017; Shaikh et al. 2018). Out of these, magnetic clouds have slowly varying magnetic fields, low plasma temperature, plasma beta, and dynamic pressure whereas ICME sheaths often have highly fluctuating fields and high plasma temperature, plasma beta, and dynamic pressure (Choe et al. 1992; Farrugia et al. 1993; Tsurutani & Gonzalez 1995; Gonzalez et al. 1999; Pulkkinen et al. 2007). In contrast, i.e. during the solar minimum, polar coronal holes are dominant and play a major role in interplanetary space (Gonzalez et al. 1999; Tsurutani et al. 2006a). Coronal holes generate regions of high speed streams (HSSs) (Sheeley, Harvey & Feldman 1976; Burlaga & Lepping 1977; Phillips et al. 1995; Gonzalez et al. 1999; Tsurutani et al. 2006a). Their interaction with slow solar wind streams induces corotating interaction regions (CIRs) whose further interaction with the magnetosphere causes weaker and moderate recurrent geomagnetic storms (Sharp, Johnson & Shelley 1976; Burlaga & Lepping 1977; Tsurutani et al. 1995b; Gonzalez et al. 1999; De Lucas et al. 2007; Echer et al. 2008; Yermolaev et al. 2018). In summary, the literature suggests that the CIRs and ICME substructures (i.e. magnetic cloud and shock-sheath) are the major drivers of geomagnetic storms; see the papers, for instance, by Tsurutani & Gonzalez (1997), Gonzalez et al. (1999), Zhang et al. (2007), Yermolaev et al. (2010a), Tsurutani & Gonzalez (1997), Gonzalez et al. (1999), Yermolaev & Yermolaev (2006), Zhang et al. (2007), Turner et al. (2009), Yermolaev et al. (2012b, 2010b, 2011), Nikolaeva, Yermolaev & Lodkina (2011), Gonzalez et al. (2011), Guo et al. (2011) and references therein.

The geomagnetic storm profiles are separated into three different phases. The storm usually starts with a sudden increase in the Earth's magnetic field considered as sudden shock commencement or initial phase. The interval of a large decrease in the *Dst*/SYM-H index represents the main phase, i.e. the period following the initial phase, which is usually of few hours to one day (Dessler & Parker 1959; Gonzalez et al. 1994). The main phase is followed by a recovery phase in which the Earth's magnetic field return to normal conditions. This is the relief of the main phase stress through the transfer of energy of trapped protons to the neutral atmospheric hydrogen atoms, i.e. an ion–atom charge exchange process (Dessler & Parker 1959). However, it is important to note that storm recovery is a highly complex mechanism in which one side of the ring current loses its particles via the charge exchange process, wave–particle interactions, Coulomb collisions etc. and, on the other hand, there is continuous particle/energy pumping into the ring current, which extends the recovery phase of the storm (Gonzalez et al. 1994; Fok et al. 1995; Jordanova et al. 1997; Miyoshi et al. 2003; Søraas et al. 2004; Tsurutani et al. 2006a; Kasahara et al. 2009).

The prediction of time corresponding to the minimum value that the *Dst* index will reach is the main goal of geomagnetic storm forecasting research. However, many technological applications rely on the expected time of the disturbed magnetosphere returning to quiet time conditions. These predictions are even more important for extreme/severe geomagnetic storms (Cid et al. 2014). In the literature, a linear proportional relation is expected between the decay rate of the ring current and the *Dst* index through the Dessler–Parker–Sckopke relationship (Olbert, Siscoe & Vasyliunas 1968; Greenspan & Hamilton 2000). Therefore, an exponential function was accepted to fit the recovery phase *Dst* index data to find the decay time of the storm (e.g. Burton, McPherron & Russell 1975; Hamilton et al. 1988; Ebihara & Ejiri 1998; O'Brien & McPherron 2000; Dasso, Gómez & Mandrini 2002; Kozyra et al. 2002; Wang, Chao & Lin 2003; Weygand & McPherron 2006; Monreal MacMahon & Llop-Romero 2008). In a few cases, the decay time was expected to be a constant value (Burton et al. 1975). Moreover, in some cases, this was dependent on the convective electric field E_y (O'Brien & McPherron 2000), or also dependent on the dynamic pressure (Wang et al. 2003). However, the intense and/or extreme storms show a two-phase recovery profile, i.e. an early fast recovery phase followed by slow recovery. Therefore, it was difficult to model the observational data assuming a unique exponential function (Akasofu, Chapman & Venkatesan 1963; Hamilton et al. 1988; Gonzalez et al. 1989; Prigancová & Feldstein 1992; Liemohn et al. 1999; Monreal MacMahon & Llop-Romero 2008). This issue was resolved by assuming a hyperbolic decay function (Aguado et al. 2010; Cid et al. 2014). In this model the entire recovery phase is dependent on two parameters, i.e. the minimum *Dst* value (Dst_0, the intensity of the storm or the value of the *Dst* index when the recovery phase starts) and the recovery time (τ_h, the time to get the value of $Dst_0/2$). A superposed epoch analysis of recovery phases of intense storms from 1963 to 2003 suggests that the hyperbolic decay function reproduces the experimental data better than the exponential function for any type of storm, which indicates a non-linear coupling between the decay rates of *Dst* and *Dst* (Aguado et al. 2010; Cid et al. 2014).

Generally, the recovery phase takes one to two days or sometimes more than two days, depending on the source of the magnetic storm (Dessler & Parker 1959; Gonzalez et al. 1994; Kozyra et al. 1997; Tsurutani et al. 2006a). ICMEs generate extreme storms with an exponential/hyperbolic recovery phase profile of one or two days whereas the CIR- and high-speed stream (HSS)-driven magnetic storms can last from a few days up to a few weeks (Tsurutani et al. 2006a; Aguado et al. 2010). The Alfvénic fluctuations embedded within CIRs as well as the HSSs that trail the CIR probably trigger the magnetic reconnection between the Alfvén-wave-embedded magnetic field and the magnetospheric fields, which slowly injects solar wind energy and plasma into the magnetosphere, slowing down the recovery rate and causing the extended recovery of the storms (Tsurutani et al. 1995a, 2006a). The extended recovery phase during ICME-induced geomagnetic storms is highly intriguing. Recently, Raghav et al. (2018) observed Alfvén waves in a magnetic cloud of ICME and suggested that they significantly control the dynamics of the moderate magnetic storm (~ -30 nT) and are responsible for the extended recovery. However, the physical mechanism involved in the extended recovery of severe/extreme magnetic storms is still ambiguous. In light of the aforementioned discussion, we search for the signature of Alfvén waves in a magnetic cloud of ICME, which causes extreme geomagnetic storm events with extended recovery phases. For the selected case study, we also investigate the effect of Alfvén-wave-embedded magnetic clouds and trailing solar winds on the exponential or hyperbolic recovery profile of extreme storms.

2 EVENT DETAILS

The studied event is a severe/extreme geomagnetic storm (SYM-H = −305 nT) that occurred on 2005 May 15, which was induced by a CME eruptg on 2005 May 13 (Yurchyshyn et al. 2006). The geomagnetic pulsations are studied during the initial phase of the storm (Kozyreva & Kleimenova 2007). The ionospheric response during the storm is investigated in detail for the Brazilian sector, South African sector and Indian regional sector (Sastri, Niranjan & Subbarao 2002; De Abreu et al. 2011; Ngwira et al. 2012). Large enhancements in total electron content (TEC) are observed during the storm, which is a cause of concern for satellite-based navigation and ground positioning. Further, the modulations in TEC confirm the presence of travelling atmospheric disturbance over a wide range of longitudes (Sharma et al. 2011). In fact, the dynamics of energetic electrons and protons of the outer radiation belt during the storm is analysed (Tverskaya et al. 2007).

Fig. 1 demonstrates the temporal evolution of the interplanetary magnetic field (IMF) and plasma parameters measured by the *Wind* spacecraft. The total IMF B_T, solar wind speed V_{sw} and proton density N_p show a sharp enhancement on May 15, suggesting the arrival of the shock front at the spacecraft. In general, the presence of the shock should be confirmed with the Rankine–Hugoniot relation. The CfA Interplanetary Shock Database available at https://www.cfa.harvard.edu/shocks/wi_data/00398/wi_00398.html validates the observations. In this database, various methods are utilized to estimate the shock characteristics. The average shock normal angle (θ_{Bn}) is about 82.1°. High fluctuations are observed in the IMF components, IMF orientation, plasma density and plasma β, which is interpreted as the ICME sheath region (see the pink shaded region). The excess speed of the magnetic cloud of the ICME generates the shock front whereas the sheath region develops due to the high compression of plasma between the shock front and the magnetic cloud. The slow and gradual decrease in total IMF and its components, slow rotation of IMF orientation, gradual and steady decrease in solar wind speed, and proton density and low plasma β are characteristics of a magnetic cloud of the ICME that are clearly seen in Fig. 1 (see the cyan shaded region). A sharp enhancement is also observed in the SYM-H index with approximately half an hour of delay with the shock front, which is explained on the basis of the distance of the spacecraft from the bow-shock of the Earth, which is further interpreted as a sudden commencement of shock. The sharp and step decrease to −305 nT is observed in the SYM-H index associated with the onset of a magnetic cloud. This indicates the main phase of the extreme geomagnetic storm. The main phase is followed by a fast recovery up to −165 nT within ∼2.5 h. However, the recovery rate suddenly slowed down to ∼0.76 nT h^{-1} (the rate is estimated for the 2005 May 16–20 SYM-H data) such that the complete recovery lasted for ∼4.5 d, which leads to the long-duration strong, moderate and weak storm-like conditions.

3 IDENTIFICATION OF THE ALFVÉN WAVE

Non-compressible magnetohydrodynamic fluctuations, i.e. Alfvén waves, are primal fluctuations in magnetized plasma. In this, the magnetic field and particle fluctuations are perpendicular to the background field direction and their motion is along the magnetic field tension force. The recent work associated with Alfvén waves in the solar wind employed the Walén relation to identify them, which is described as (Walén 1944; Hudson 1971)

$$V_A = \pm A \frac{B}{\sqrt{\mu_0 \rho}} \quad (1)$$

where A is the anisotropy parameter, B is the magnetic field vector and ρ is the proton mass density. In the solar wind, the negligible thermal anisotropy leads to $A = \pm 1$ (Yang et al. 2016; Raghav et al. 2018; Raghav & Kule 2018a,b).

In the Walén test, proper estimation of the background magnetic field is important. However, this is not an observable quantity and therefore the average value of the de Hoffmann–Teller (HT) frame or the mean value of the magnetic field is utilized (Gosling, Teh & Eriksson 2010; Yang & Chao 2013; Raghav & Kule 2018a,b; Raghav et al. 2018). However, the HT frame can change in high-speed solar wind streams and the solar wind fluctuations are pertinent to a slowly varying base value of the magnetic field (Gosling et al. 2009; Li et al. 2016). Therefore, to minimize the uncertainties in Alfvén wave identification, we apply bandpass filters to the plasma velocity and magnetic field observations. 10 evenly divided logarithmic frequency bands are selected. The possible filters are 10–15 s, 15–25 s, 25–40 s, 40–60 s, 60–100 s, 100–160 s, 160–250 s, 250–400 s, 400–630 s and 630–1000 s. The Walén relation for each bandpassed signal is diagnosed as follows:

$$V_i = \pm V_{Ai}. \quad (2)$$

Here V_i and V_{Ai} are the bandpassed V and V_A components with the ith filter. The significant value of the correlation coefficient of the respective components of V_i and V_{Ai} confirms the existence of Alfvén waves or Alfénic fluctuations in the region of examination. The + or − signs express the propagation parallel and anti-parallel to the background magnetic field, respectively. A similar approach is utilized by Li et al. (2016). The complete region under study is divided into subregions (each with a 30 min time window). Fig. 2 show a contour plot of the frequency–time distribution with a bin size of 30 min. Here, the absolute value of the correlation coefficient of each subregion is displayed as a colour map on the contour plot. Correlation coefficients >0.65 are included in the map whereas lower values are explicitly discarded. Therefore, the colour strips in the contour map of Fig. 2 represent the existence of dominant Alfvénic flow along the x-, y- and z-components.

4 RESULTS

Here, we studied the extreme geomagnetic storm (SYM-H(min) = −305 nT) induced by ICME. Generally, ICME-generated geomagnetic storm recovery phases are of few hours to a maximum of one day or rarely two days (Tsurutani et al. 2006a), but we observed an extended recovery phase for the extreme storm, i.e. ∼4.5 d. Interestingly, we noticed correlated variations in the magnetic and solar wind velocity components (not shown here). A detailed investigation employing filters for the velocity and magnetic field observations indicates the presence of Alfvén waves in the magnetic cloud corresponding to the extended recovery phase. Alfvénic fluctuations are identified in the solar wind, i.e. well before the onset of shock. It is important to note that the Alfvénic fluctuations are weak or absent in the ICME sheath region (on 2005 May 15, 2:40 to 06:18 UT) and at the front edge of the magnetic cloud region (on 2005 May 15, 06:18 to 10:00 UT). As the magnetic cloud crosses the spacecraft, the Alfvénic nature in the lower-frequency domain significantly enhanced. Strong Alfvénic *behaviour* is clearly observed from 2005 May 17–20. However, for small time intervals the Alfvénic nature reduces. Certainly, it appears that the Alfvénic nature is dominant in the trailing solar wind as well. The SYM-H index variations show a gradual recovery corresponding to the interplanetary region in which the Alfvénic fluctuations are present either weakly and/or strongly. Here we opine that, in the current analysis, the frequency domain between 10^{-1} and 10^{-3} Hz is considered. However, lower-frequency domains, i.e. high-wavelength Alfvén waves, are not considered. Fig. 2 also indicates that, in regions that display weak Alfvén fluctuations, the Alfvénicity is increased from the higher-frequency to the lower-frequency domain. It is also possible that lower-frequency Alfvén waves may exist throughout the magnetic cloud.

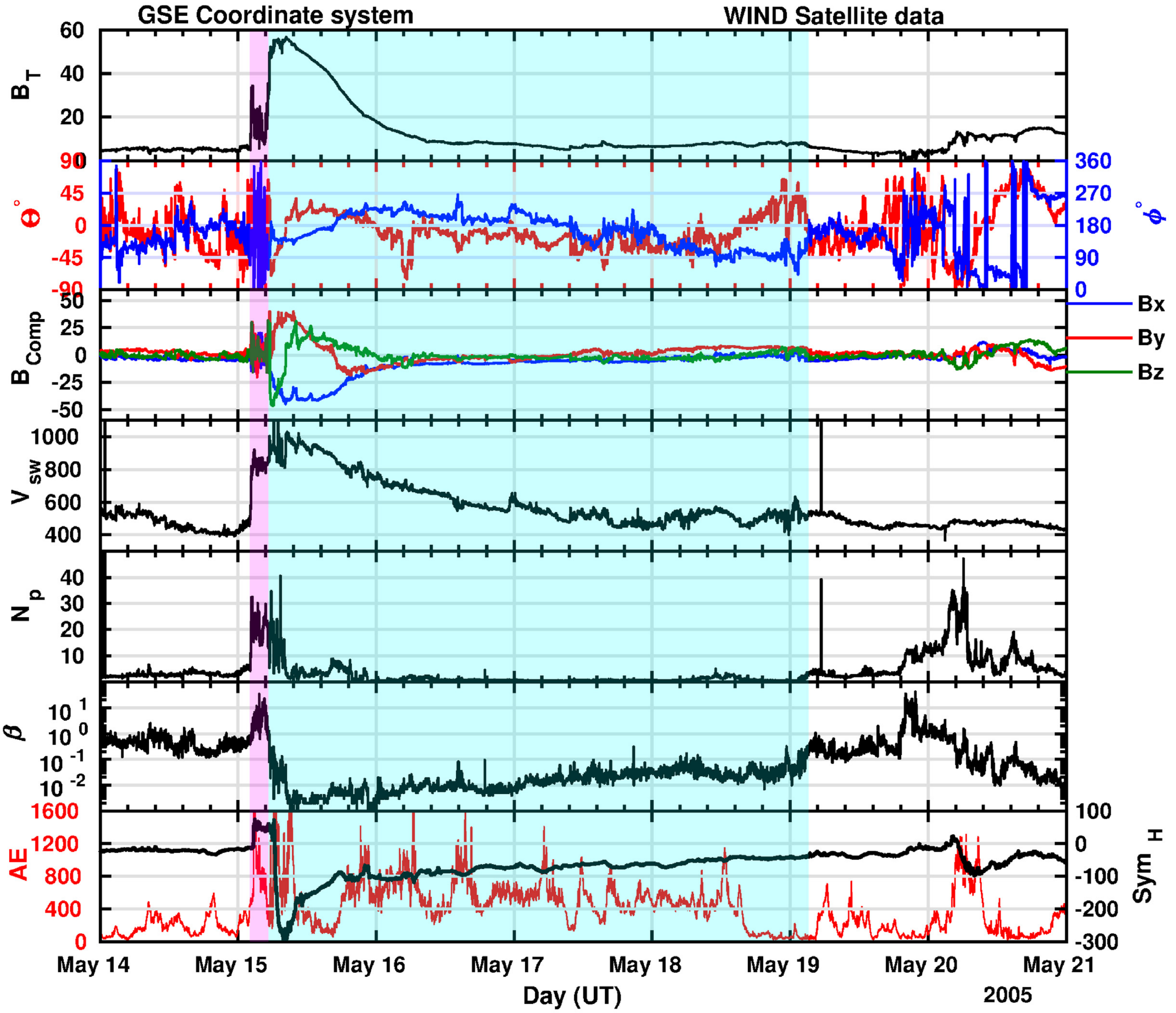

Figure 1. From top to bottom, the first panel shows the magnetic field strength ($|B|$), the second panel shows the angle θ and ϕ. The third, fourth, and fifth panels show the vector components of the magnetic field, solar wind speed and proton density in the GSE coordinate system respectively. The sixth panel shows the plasma beta profile (data taken from the *Wind* satellite with a time cadence of 92 s). The bottom panel shows the SYM-H and AE indexes (data taken from the OMNI database with 60 s time resolution). The pink shaded region represents the ICME sheath and the cyan shaded region is the magnetic cloud of the ICME.

5 MODEL FIT

The studied storm event demonstrates two phase recovery profiles, i.e. fast and slow. To study the features of the extended recovery profile, exponential decay, hyperbolic decay, and linear (constant decay rate) equations were fitted to the recovery phase of the storm as suggested in the literature (see top panel of Fig. 3). The fast recovery phase of the storm is clearly replicated by the exponential as well as hyperbolic decay functions; however, both of the functions significantly deviated from the actual data during the slow recovery phase (see bottom panel of Fig. 3). The value of τ for exponential decay is 11.11 h whereas for hyperbolic decay it is 9.09 h. The τ value for exponential decay represents the time required to reduce the initial value of the *Dst* index (minimum value) to its $1/e$ value. Moreover, the τ value for hyperbolic decay represents the time required to reduce the initial value of the *Dst* index to its 1/2 value. This implies that the derived values of τ using both the functions are consistent with each other during the fast recovery phase. The maximum deviation for exponential decay is ∼100 per cent whereas that for hyperbolic decay is more than ∼50 per cent during the slow recovery phase. A constant recovery rate, i.e. 0.79 nT h^{-1} (linear fit), is clearly observed during the slow recovery phase with minimum deviation as compared to the other two decay functions. The significant deviation of any of the decay functions in the slow recovery phase implies that there would be either a constant plasma energy/particle injection to the magnetosphere or a physical mechanism that slows down the decay rate of the ring current. We believe that the identification of Alfvén waves corresponding to the slow recovery phase could be a possible source. More detailed study is needed in this direction. Moreover, we have also found similar extended recovery during the extreme

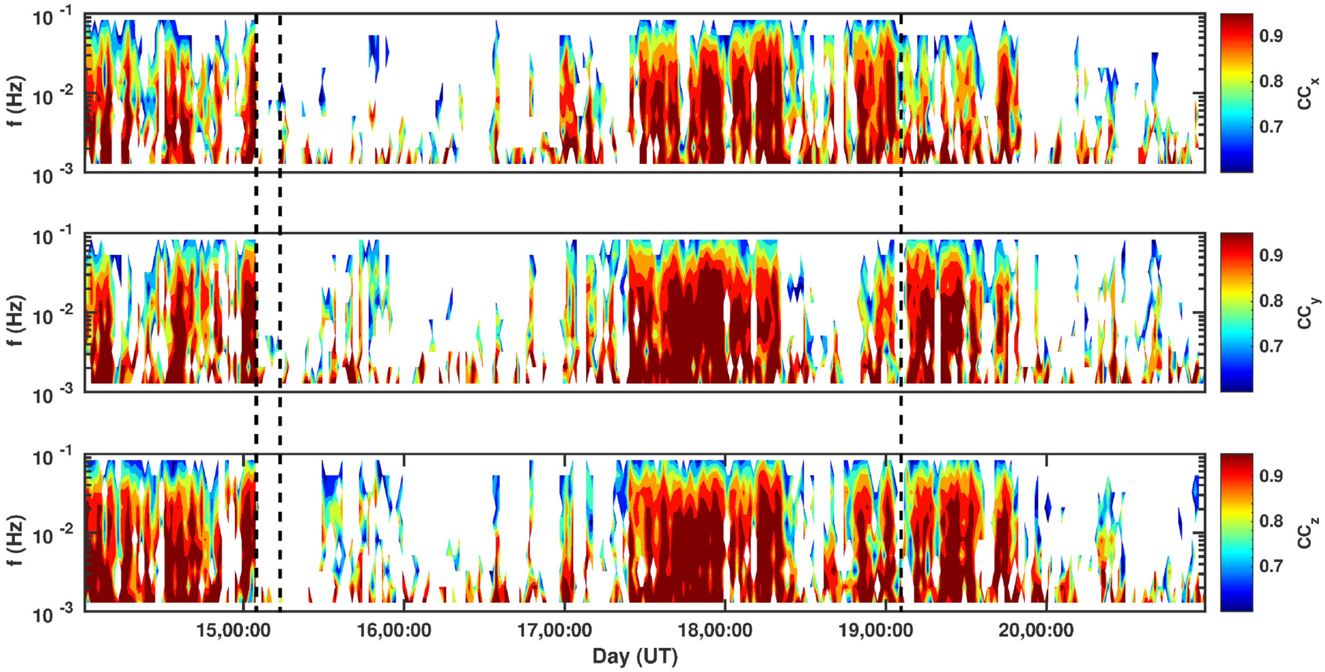

Figure 2. Frequency–time distribution of correlation coefficients between V_{Ai} and V_i for the complete event. The vertical dashed lines indicate the ICME sheath and magnetic cloud boundaries. The *Wind* satellite 3 s observations are utilized for the analysis.

storms that occurred on 2015 March 17 and 2014 June 26 (not shown here).

6 DISCUSSION AND CONCLUSION

In a geomagnetic storm, ring current formation and decay is the key element (Daglis et al. 1999; Keika et al. 2006). The solar wind and terrestrial ionosphere are the ultimate main sources of ring current particles (Stern 2005). Prominently, ring current decay occurs due to charge exchange with exospheric neutrals, wave–particle interaction and Coulomb collisions with thermal plasma (Daglis et al. 1996; Keika et al. 2006; Yermolaev et al. 2012a). Since neutralized ring current particles can escape the inner magnetosphere trapping region, charge exchange acts as a major loss mechanism for the ring current and it must be carefully considered in any ring current decay model (Daglis et al. 1999; Keika et al. 2006). Intense plasma waves provide a mechanism for energy transfer between various components of plasma. Moreover, thermal heavy ion plasma and Alfvén waves are particularly important for the heating mechanism (Gendrin & Roux 1980; Horne & Thorne 1997; Mauk 1982; Anderson & Fuselier 1994). In fact, polar observations by W1 provide evidence that the Alfvénic Poynting flux is responsible for transferring the power needed for acceleration of all the energized auroral particle populations accelerated into the ionosphere and also streaming out into the magnetosphere (Volokitin & Dubinin 1989; Wygant et al. 2002). Besides this, high-speed stream/CIR-induced magnetic storms show long recovery phases, in which it is suggested that the sporadic electron injections sustaining the ring current are driven by Alfvén waves (Tsurutani et al. 2006a; Kasahara et al. 2009). Moreover, Raghav et al. (2018) suggest that Alfvén waves embedded in ICME magnetic clouds are also responsible for the extended recovery of moderate geomagnetic storms. In light of the aforementioned result and discussion, the present study clearly demonstrates that the presence of Alfvénic fluctuations can also slow down the recovery of an extreme/severe storm (considering the analogy with past reported studies), which drastically increases the geomagnetic storm threat from all perspectives.

Storms with long recovery phases could be accounted for in another special category, i.e. high-intensity long-duration continuous AE activity (HILDCAA) events (Tsurutani & Gonzalez 1987; Tsurutani et al. 2006a; Guarnieri et al. 2006). There are conditions for the identification of HILDCAA events, i.e. the AE index must reach at least 1000 nT, it should not fall below 200 nT for more than 2 h and the condition must persist for at least two days (not considering the main phases of magnetic storms). HILDCAA events are associated with the generation of magnetospheric relativistic electron acceleration (Paulikas & Blake 1979; Baker et al. 1986; Meredith et al. 2003; Tsurutani et al. 2006a,b; Hajra et al. 2013, 2014a,b). Most of these events occur in the recovery phase of CIR-generated storms and comparatively very few events occur in ICME-induced events (Guarnieri et al. 2006; Hajra et al. 2014b). Our study also indicates that the present ICME event is also a possible candidate for an HILDCAA event (see AE index in Fig. 1).

7 IMPORTANCE AND IMPLICATIONS

The investigation of the extended recovery phase of the storm is important and has strong implications. During the magnetically disturbed period, the flux of relativistic electrons (energy range MeV) shows dynamic variations (Daglis et al. 1999). There are arguments that particles are not produced by the main phase but by the extended recovery phase (Daglis et al. 1999; Miyoshi et al. 2003). In fact, atmospheric losses of relativistic electrons are more intense during long recovery phases than fast recovery phases (Sandanger et al. 2009; Wang et al. 2016). Besides this, high-*m* poloidal waves are observed during the recovery phase of the 2015 June 22 magnetic storm (Le et al. 2017). These waves can exchange energy with energetic particles and therefore are important

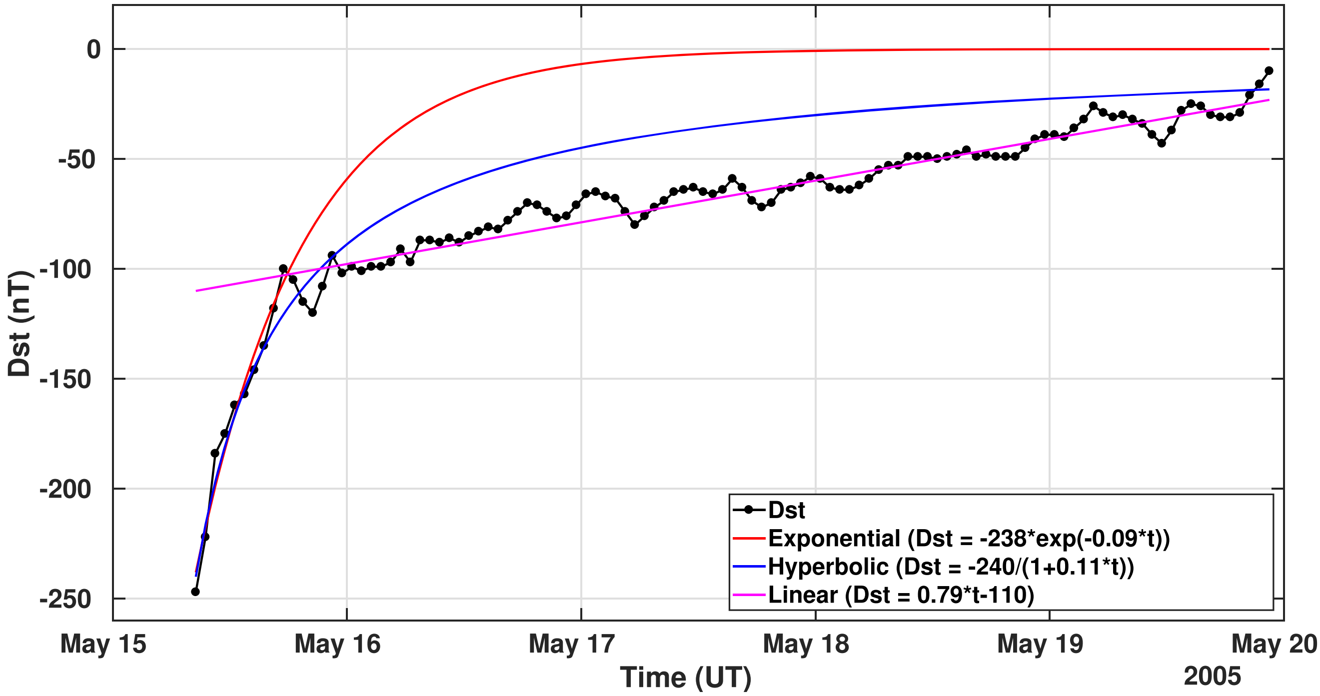

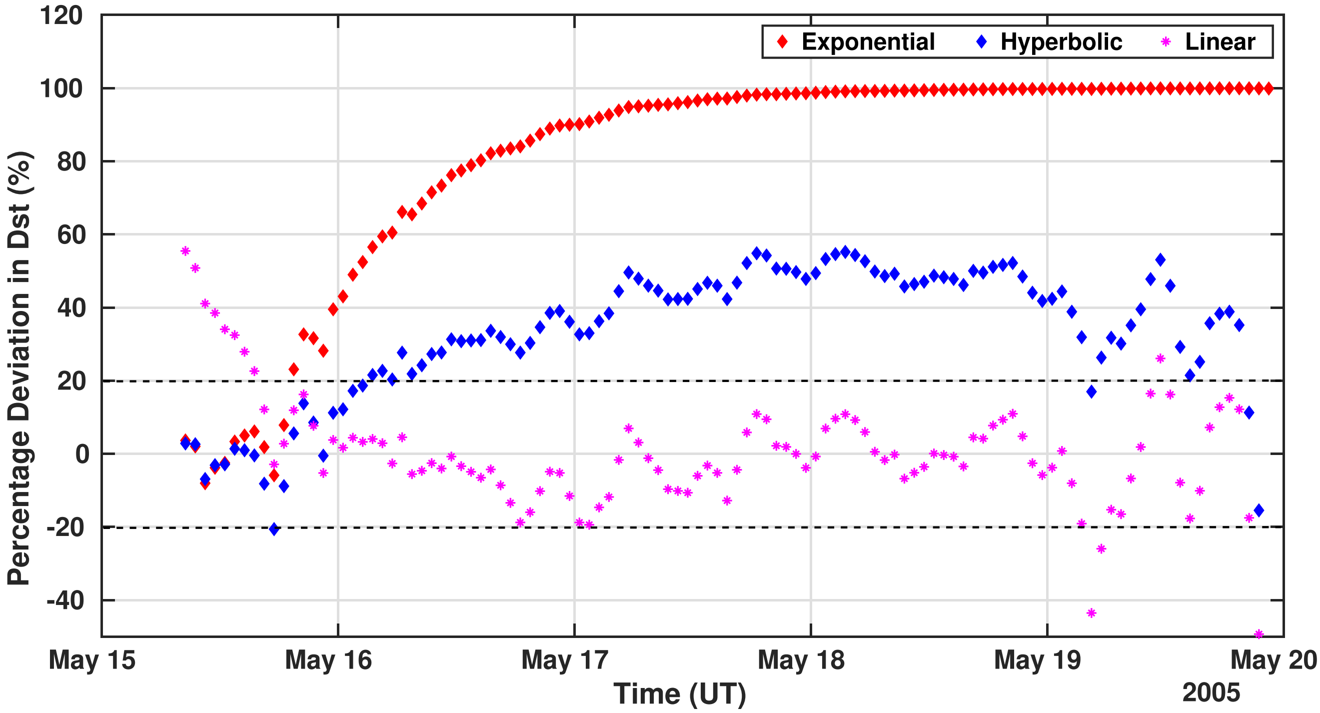

Figure 3. The top panel shows the temporal variation of the *Dst* index with exponential, hyperbolic and linear fitting of the recovery phase of the studied storm. The bottom panel demonstrates the deviation of each model-fitted value from the observational *Dst* index.

to the dynamics of the inner magnetosphere (Zong et al. 2009; Le et al. 2017). Electromagnetic ion cyclotron (EMIC) waves occur during the main phase as well as in the recovery phase of the storms (Cornwall, Coroniti & Thorne 1970; Kawamura et al. 1982; Fraser & Nguyen 2001; Denton, Jordanova & Fraser 2014; Wang et al. 2016). The geomagnetic pulsations PC1 and PC2 are rarely observed on the ground during the main and early recovery phases but, as the recovery phase progresses, these waves are increasingly observed (Engebretson et al. 2008; Wang et al. 2016).

We opine that magnetosphere investigation during similar interplanetary conditions may unfold the mystery of how Alfvénic fluctuations affect the ring current acceleration and decay processes. We will definitely pursue this investigation in the future. In Alfvén waves, plasma particles move along field lines; therefore, we opine that interplanetary field reconnection with Earth's magnetic field provides direct access to plasma particles with minimum resistance (which possibly advance the particle diffusion in a magnetic field) even though B_z fluctuates near zero. In summary, we suggest that extreme/severe storms create hazardous scenarios in many ways and their extended recovery phase adds burning fuel to this. There are various physical phenomena that materialize during the recovery phase of magnetic storms, establishing the importance of the present study.

ACKNOWLEDGEMENTS

The authors are grateful to Lynn B. Wilson III for providing *Wind* spacecraft data (wind.nasa.gov). The authors are also grateful to CDAWeb for making the interplanetary, SYM-H and AE index data available. We also acknowledge the CfA Interplanetary Shock Database.

REFERENCES

Aguado J., Cid C., Saiz E., Cerrato Y., 2010, J. Geophysical Res. Space Phys., 115, A07220
Akasofu S.-I., 1981, Space Sci. Rev., 28, 121
Akasofu S.-I., Chapman S., Venkatesan D., 1963, J. Geophysical Res., 68, 3345
Anderson B., Fuselier S., 1994, J. Geophysical Res. Space Phys., 99, 19413
Baker D., Blake J. B., Klebesadel R., Higbie P. R., 1986, J. Geophysical Res. Space Phys., 91, 4265
Burlaga L., Lepping R., 1977, Planet. Space Sci., 25, 1151
Burton R. K., McPherron R., Russell C., 1975, J. Geophysical Res., 80, 4204
Chapman S., Bartels J., 1940, Geomagnetism, Vol. 2. Clarendon Press, Oxford
Choe G., LaBelle-Hamer N., Tsurutani B., Lee L., 1992, Eos Trans. AGU, 73, 485
Cid C., Palacios J., Saiz E., Guerrero A., Cerrato Y., 2014, J. Space Weather Space Climate, 4, A28
Cornwall J. M., Coroniti F. V., Thorne R. M., 1970, J. Geophysical Res., 75, 4699
Daglis I. A., Axford W. I., Livi S., Wilken B., Grande M., Søraas F., 1996, J. Geomagnetism Geoelectricity, 48, 729
Daglis I. A., Thorne R. M., Baumjohann W., Orsini S., 1999, Rev. Geophysics, 37, 407
Dasso S., Gómez D., Mandrini C. H., 2002, J. Geophysical Res. Space Phys., 107, A2, SMP–05
De Abreu A., Sahai Y., Fagundes P., De Jesus R., Bittencourt J., Pillat V., 2011, Advances Space Res., 48, 1211
De Lucas A., Gonzalez W., Echer E., Guarnieri F., Dal Lago A., Da Silva M., Vieira L., Schuch N., 2007, J. Atmos. Sol.-Terr. Phys., 69, 1851
Denton R., Jordanova V. K., Fraser B., 2014, J. Geophysical Res. Space Phys., 119, 8372
Dessler A. J., Parker E. N., 1959, J. Geophysical Res., 64, 2239
Dungey J. W., 1961, Phys. Rev. Lett., 6, 47
Ebihara Y., Ejiri M., 1998, Geophysical Res. Lett., 25, 3751
Echer E., Gonzalez W., 2004, Geophysical Res. Lett., 31, 9
Echer E., Gonzalez W., Guarnieri F., Dal Lago A., Vieira L., 2005a, Advances Space Res., 35, 855
Echer E., Gonzalez W., Tsurutani B., Vieira L., Alves M., Gonzalez A., 2005b, J. Geophysical Res. Space Phys., 110, A2
Echer E., Gonzalez W., Tsurutani B., Gonzalez A., 2008, J. Geophysical Res. Space Phys., 113, A5
Engebretson M. et al., 2008, J. Geophysical Res. Space Phys., 113, A7
Farrugia C., Burlaga L., Osherovich V., Richardson I., Freeman M., Lepping R., Lazarus A., 1993, J. Geophysical Res. Space Phys., 98, 7621
Fok M.-C., Craven P. D., Moore T. E., Richards P. G., 1995, in Horwitz J. L., Singh N., Burch J. L.eds, Cross-scale coupling in space plasmas, Volume 93. American Geophysical Union (AGU), Florida Aveneu, N.W. Washington, DC 20009, p. 161
Förster M., Jakowski N., 2000, Surv. Geophysics, 21, 47
Foster J., Tetenbaum D., 1991, J. Geophysical Res. Space Phys., 96, 1251
Fraser B., Nguyen T., 2001, J. Atmos. Sol.-Terr. Phys., 63, 1225
Gendrin R., Roux A., 1980, J. Geophysical Res. Space Phys., 85, 4577
Gonzalez W., Mozer F., 1974, J. Geophysical Res., 79, 4186
Gonzalez W. D., Tsurutani B. T., 1987, Planet. Space Sci., 35, 1101
Gonzalez W. D., Tsurutani B. T., Gonzalez A. L., Smith E. J., Tang F., Akasofu S.-I., 1989, J. Geophysical Res. Space Phys., 94, 8835
Gonzalez W., Joselyn J., Kamide Y., Kroehl H., Rostoker G., Tsurutani B., Vasyliunas V., 1994, J. Geophysical Res. Space Phys., 99, 5771
Gonzalez W. D., Tsurutani B. T., De Gonzalez A. L. C., 1999, Space Sci. Rev., 88, 529
Gonzalez W. D., Echer E., Tsurutani B. T., de Gonzalez A. L. C., Dal Lago A., 2011, Space Sci. Rev., 158, 69
Gosling J., McComas D., Roberts D., Skoug R., 2009, ApJ, 695, L213
Gosling J., Teh W.-L., Eriksson S., 2010, ApJ, 719, L36
Greenspan M., Hamilton D., 2000, J. Geophysical Res. Space Phys., 105, 5419
Guarnieri F. L., Tsurutani B. T., Gonzalez W. D., Echer E., Gonzalez A. L., Grande M., Soraas F., 2006, in Gopalswamy N., Bhattacharyya A., eds, ILWS Workshop. Goa, India
Guo J., Feng X., Emery B. A., Zhang J., Xiang C., Shen F., Song W., 2011, J. Geophysical Res. Space Phys., 116, A5
Hajra R., Echer E., Tsurutani B., Gonzalez W., 2013, J. Geophysical Res. Space Phys., 118, 5626
Hajra R., Echer E., Tsurutani B. T., Gonzalez W. D., 2014a, J. Geophysical Res. Space Phys., 119, 2675
Hajra R., Echer E., Tsurutani B. T., Gonzalez W. D., 2014b, J. Atmos. Sol.-Terr. Phys., 121, 24
Hamilton D. C., Gloeckler G., Ipavich F., Stüdemann W., Wilken B., Kremser G., 1988, J. Geophysical Res. Space Phys., 93, 14343
Horne R. B., Thorne R. M., 1997, J. Geophysical Res. Space Phys., 102, 11457
Hudson P., 1971, Planet. Space Sci., 19, 1693
Huttunen K., Koskinen H., Karinen A., Mursula K., 2006, Geophysical Res. Lett., 33, 6
Jordanova V., Kozyra J., Nagy A., Khazanov G., 1997, J. Geophysical Res. Space Phys., 102, 14279
Kasahara Y., Miyoshi Y., Omura Y., Verkhoglyadova O., Nagano I., Kimura I., Tsurutani B., 2009, Geophysical Res. Lett., 36, 1
Kawamura M., Kuwashima M., Toya T., 1982, (3-16)
Keika K., Nosé M., Brandt P., Ohtani S., Mitchell D., Roelof E., 2006, J. Geophysical Res. Space Phys., 111, A11
Kozyra J., Jordanova V., Home R., Thorne R., 1997, in Tsurutani B. T., Gonzalez W. D., Kamide Y., Arballo J. K., eds, Magnetic storms, 98. American Geophysical Union (AGU), Florida Aveneu, N.W. Washington, DC 20009, p. 187
Kozyra J. et al., 2002, J. Geophysical Res. Space Phys., 107, A8, SMP–33
Kozyreva O., Kleimenova N., 2007, Geomagnetism Aeronomy, 47, 470
Laštovička J., 1996, J. Atmos. Terr. Phys., 58, 831
Le G. et al., 2017, Geophysical Res. Lett., 44, 3456
Li H., Wang C., Chao J., Hsieh W., 2016, J. Geophysical Res. Space Phys., 121, 42
Liemohn M., Kozyra J., Jordanova V., Khazanov G., Thomsen M., Cayton T., 1999, Geophysical Res. Lett., 26, 2845
Mauk B., 1982, Geophysical Res. Lett., 9, 1163
Meredith N. P., Cain M., Horne R. B., Thorne R. M., Summers D., Anderson R. R., 2003, J. Geophysical Res. Space Phys., 108, A8
Miyoshi Y., Morioka A., Misawa H., Obara T., Nagai T., Kasahara Y., 2003, J. Geophysical Res. Space Phys., 108, A1
Monreal MacMahon R., Llop-Romero C., 2008, Ann. Geophysicae, 26, 2543
Ngwira C. M., McKinnell L.-A., Cilliers P. J., Yizengaw E., 2012, Advances Space Res., 49, 327
Nikolaeva N., Yermolaev Y. I., Lodkina I., 2011, Geomagnetism Aeronomy, 51, 49

O'Brien T. P., McPherron R. L., 2000, J. Geophysical Res. Space Phys., 105, 7707
Olbert S., Siscoe G., Vasyliunas V., 1968, J. Geophysical Res., 73, 1115
Oughton E. J., Skelton A., Horne R. B., Thomson A. W., Gaunt C. T., 2017, Space Weather, 15, 65
Paulikas G., Blake J., 1979, in Olson W. P., ed., Quantitative modeling of magnetospheric processes, vol. 21. American Geophysical Union (AGU), Florida Aveneu, N.W. Washington, DC 20009, p. 180
Phillips J. et al., 1995, Science, 268, 1030
Prigancová A., Feldstein Y. I., 1992, Planet. Space Sci., 40, 581
Pulkkinen T. I., Partamies N., Huttunen K., Reeves G., Koskinen H., 2007, Geophysical Res. Lett., 34, L02105
Raghav A. N., Kule A., 2018a, MNRAS, 476, L6
Raghav A. N., Kule A., 2018b, MNRAS, 480, L6
Raghav A., Bhaskar A., Lotekar A., Vichare G., Yadav V., 2014, J. Cosmology Astroparticle Phys., 2014, 074
Raghav A., Shaikh Z., Bhaskar A., Datar G., Vichare G., 2017, Sol. Phys., 292, 99
Raghav A. N., Kule A., Bhaskar A., Mishra W., Vichare G., Surve S., 2018, ApJ, 860, 26
Rao P. R., Krishna S. G., Prasad J. V., Prasad S., Prasad D., Niranjan K., 2009, Ann. Geophysicae, 27, 2101
Rostoker G., Fälthammar C. G., 1967, J. Geophysical Res., 72, 5853
Sandanger M., Søraas F., Sørbø M., Aarsnes K., Oksavik K., Evans D., 2009, J. Atmos. Sol.-Terr. Phys., 71, 1126
Sastri J. H., Niranjan K., Subbarao K., 2002, Geophysical Res. Lett., 29, 29
Shaikh Z., Raghav A., Bhaskar A., 2017, ApJ, 844, 121
Shaikh Z. I., Raghav A. N., Vichare G., Bhaskar A., Mishra W., 2018, ApJ, 866, 118
Sharma S., Galav P., Dashora N., Pandey R., 2011, Ann. Geophysicae, 29, 1063
Sharp R., Johnson R., Shelley E., 1976, J. Geophysical Res., 81, 3292
Sheeley N., Harvey J., Feldman W., 1976, Sol. Phys., 49, 271
Shelley E. G., Johnson R., Sharp R., 1972, J. Geophysical Res., 77, 6104
Søraas F., Aarsnes K., Oksavik K., Sandanger M., Evans D., Greer M., 2004, J. Atmos. Sol.-Terr. Phys., 66, 177
Stern D. P., 2005, The Inner Magnetosphere: Physics and Modeling. p. 1
Thomson A. W., McKay A. J., Clarke E., Reay S. J., 2005, Space Weather, 3, 1
Tsurutani B. T., Gonzalez W. D., 1987, Planet. Space Sci., 35, 405
Tsurutani B., Gonzalez W., 1995, J. Atmos. Terr. Phys., 57, 1369
Tsurutani B. T., Gonzalez W. D., 1997, in Tsurutani B. T., Gonzalez W. D., Kamide Y., Arballo J. K., eds, Magnetic storms, vol. 98. American Geophysical Union (AGU), Florida Aveneu, N.W. Washington, DC 20009, p. 77
Tsurutani B. T., Gonzalez W. D., Tang F., Akasofu S. I., Smith E. J., 1988, J. Geophysical Res. Space Phys., 93, 8519
Tsurutani B. T., Gonzalez W. D., Tang F., Lee Y. T., 1992, Geophysical Res. Lett., 19, 73
Tsurutani B. T., Ho C. M., Arballo J. K., Goldstein B. E., Balogh A., 1995a, Geophysical Res. Lett., 22, 3397
Tsurutani B. T., Gonzalez W. D., Gonzalez A. L., Tang F., Arballo J. K., Okada M., 1995b, J. Geophysical Res. Space Phys., 100, 21717
Tsurutani B. T. et al., 2006a, J. Geophysical Res. Space Phys., 111, A07S01
Tsurutani B. T., McPherron R. L., Gonzalez W. D., Lu G., Gopalswamy N., Guarnieri F. L., 2006b, in Tsurutani B., McPherron R., Lu G., Sobral J. H. A., eds, Recurrent magnetic storms: corotating solar wind streams, vol. 167. American Geophysical Union (AGU), Florida Aveneu, N.W. Washington, DC 20009, p. 1
Turner N. E., Cramer W. D., Earles S. K., Emery B. A., 2009, J. Atmos. Sol.-Terr. Phys., 71, 1023
Tverskaya L., Ginzburg E., Ivanova T., Pavlov N., Svidsky P., 2007, Geomagnetism Aeronomy, 47, 696
Volokitin A., Dubinin E., 1989, Planet. Space Sci., 37, 761
Walén C., 1944, Arkiv Astron., 30, 1
Wang C., Chao J., Lin C.-H., 2003, J. Geophysical Res. Space Phys., 108, A9
Wang D., Yuan Z., Yu X., Huang S., Deng X., Zhou M., Li H., 2016, J. Geophysical Res. Space Phys., 121, 6444
Weygand J. M., McPherron R. L., 2006, J. Geophysical Res. Space Phys., 111, A11221
Wygant J. et al., 2002, J. Geophysical Res. Space Phys., 107, A8
Yang L., Chao J., 2013, Chinese J. Space Sci, 33, 353
Yang L., Lee L., Chao J., Hsieh W., Luo Q., Li J., Shi J., Wu D., 2016, ApJ, 817, 178
Yermolaev Y. I., Yermolaev M. Y., 2006, Advances Space Res., 37, 1175
Yermolaev Y. I., Lodkina I. G., Nikolaeva N. S., Yermolaev M. Y., 2010a, Cosmic Res., 48, 485
Yermolaev Y. I., Nikolaeva N. S., Lodkina I. G., Yermolaev M. Y., 2010b, in Maksimovic M., Issautier K., Meyer-Vernet N., Moncuquet M., Pantellini F., eds, Twelfth International Solar Wind Conference. AIP Conference Proceedings, Saint-Malo (France), p. 648
Yermolaev Y. I., Lodkina I., Nikolaeva N., Yermolaev M. Y., 2011, Cosmic Res., 49, 21
Yermolaev Y. I., Lodkina I., Nikolaeva N., Yermolaev M. Y., 2012a, J. Geophysical Res. Space Phys., 117, A00L07
Yermolaev Y. I., Nikolaeva N., Lodkina I., Yermolaev M. Y., 2012b, J. Geophysical Res. Space Phys., 117
Yermolaev Y. I., Lodkina I., Nikolaeva N., Yermolaev M. Y., Riazantseva M., Rakhmanova L., 2018, J. Atmos. Sol.-Terr. Phys., 1
Yurchyshyn V., Liu C., Abramenko V., Krall J., 2006, Sol. Phys., 239, 317
Zhang J. et al., 2007, J. Geophysical Res. Space Phys., 112, A10102
Zong Q.-G. et al., 2009, J. Geophysical Res. Space Phys., 114, A10204

This paper has been typeset from a TEX/LATEX file prepared by the author.